AAPS PharmSciTech, Vol. 10, No. 1, March 2009 (© 2009)
DOI: 10.1208/s12249-008-9183-0

Research Article

Studies on Mefenamic Acid Microparticles: Formulation, *In Vitro* Release, and *In Situ* Studies in Rats

Ferhan Sevgi,[1,3] Aysu Yurdasiper,[1] Buket Kaynarsoy,[1] Ezgi Turunç,[2] Tamer Güneri,[1] and Ayfer Yalçın[2]

Received 11 July 2008; accepted 13 December 2008; published online 29 January 2009

Abstract. In this study, we investigated the *in vitro* characteristics of mefenamic acid (MA) microparticles as well as their effects on DNA damage. MA-loaded chitosan and alginate beads were prepared by the ionotropic gelation process. Microsponges containing MA and Eudragit RS 100 were prepared by quasi-emulsion solvent diffusion method. The microparticles were characterized in terms of particle size, surface morphology, encapsulation efficiency, and *in vitro* release profiles. Most of the formulation variables manifested an influence on the physical characteristics of the microparticles at varying degrees. We also studied the effects of MA, MA-loaded microparticles, and three different polymers on rat brain cortex DNA damage. Our results showed that DNA damage was higher in MA-loaded Eudragit microsponges than MA-loaded biodegradable chitosan or alginate microparticles.

KEY WORDS: DNA damage; kainic acid; mefenamic acid; microparticles.

INTRODUCTION

Mefenamic acid (MA) [(2-[(2,3-dimethylphenyl)amino] benzoic acid], an anthranilic acid derivative, is a nonsteroidal anti-inflammatory (NSAI), antipyretic, and analgesic agent that is used for the relief of postoperative and traumatic inflammation and swelling, antiphlogistic and analgesic treatment of rheumatoid arthritis, and antipyretic in acute respiratory tract infection (1) (Fig. 1). Recently, it has been reported that MA could be used as a therapeutic agent in Alzheimer's disease since it improves learning and memory impairment in an amyloid β peptide (Aβ1–42)-infused Alzheimer's disease rat model (2).

Similar to other drugs of this group, MA has a wide spectrum of gastrointestinal disorders (3,4). Sustained release MA microspheres (5,6), MA matrix tablets (7,8), and controlled release MA-loaded alginate beads (9) have been reported in the literature. MA is classified as class II on the basis of the biopharmaceutical classification system (10,11) because of its poor solubility over the pH range 1.2–7.5 [solubility=0.2 μg/mL (pH 1.2), 0.12 mg/mL (pH 7.5)] (12,13) and high permeability in Caco-2 cell model (13). The usual oral dose is 250 or 500 mg, being administered three times daily (3,8). However, no commercially long-acting product exists in the market. The short biological half-life of 2 h following oral dosing necessitates frequent administration of the drug in order to maintain the desired steady state levels (3). The formulation of MA as a modified release dosage form of Eudragit microsponges seems to be an alternative approach to overcome the potential problems in the gastrointestinal tract, as it reduces the adverse effects of nonsteroidal anti-inflammatory drugs (NSAIDs) (14,15).

NSAIDs are widely used therapeutic agents that have anti-inflammatory, analgesic, and antipyretic activities. NSAIDs are involved in the suppression of prostaglandin synthesis by inhibiting cyclooxygenases, enzymes that catalyze the formation of prostaglandin precursors from arachidonic acid. It has been reported that inflammatory processes are associated with the pathophysiology of Alzheimer's disease and that treatment with NSAIDs reduces the risk of Alzheimer's disease (16).

Epidemiological observations indicate that long-term treatment of patients suffering from rheumatoid arthritis with NSAIDs results in reduced risk and delayed onset of Alzheimer's disease. Kainic acid (KA) is a glutamate agonist with relative selectivity for the *N*-methyl-D-aspartate (NMDA) receptors in the brain. It is an excitatory neurotoxic substance and stimulates NMDA receptors that results in transmembrane ion imbalance, especially causing calcium influx, which in turn stimulates reactive oxygen species (ROS) such as H_2O_2, superoxide anion ($^{\cdot}O_2^-$), and hydroxyl radical ($^{\cdot}OH$) (17,18).

The present study demonstrates, for the first time, the potential effect of MA microparticles and the polymers used in their formulations on DNA damage induced by KA as well as *in vitro* release of MA microparticles prepared by three different polymers.

We aimed to prepare modified release MA microsponges with Eudragit RS 100 polymer by using quasi-emulsion solvent diffusion (QESD) method (19–24). Microsponges are porous, polymeric microspheres that are used mostly for topical (25–28) and, recently, for oral administration (23,24,29). On the other hand, MA microparticles were prepared by using biodegradable

[1] Department of Pharmaceutical Technology, Faculty of Pharmacy, Ege University, 35100, Bornova, Izmir, Turkey.
[2] Department of Biochemistry, Faculty of Pharmacy, Ege University, 35100, Bornova, Izmir, Turkey.
[3] To whom correspondence should be addressed. (e-mail: ferhan.sevgi@ege.edu.tr)

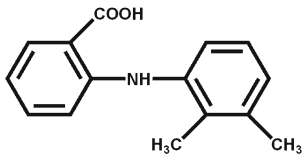

Fig. 1. Schematic of MA

and biocompatible chitosan and alginate polymers by ionotropic gelation method (9,30–32).

Eudragit RS 100 is referred to as ammoniomethacrylate copolymer and was used to prepare modified release microsponges. Eudragit RS 100, an acrylic resin, is a copolymer of acrylic and methacrylic acid esters with a low content of quaternary ammonium groups. Since Eudragit RS 100 films are only slightly permeable, drug release through the films is markedly retarded (33).

The use of natural polymers in the design of drug delivery formulation has received much attention due to their excellent biocompatibility and biodegradability (34). Among them, alginate and chitosan are very promising and have been widely exploited in the pharmaceutical industry for controlled drug release (35,36). Alginate and chitosan are biocompatible, biodegradable, and nontoxic in systemic administration. Alginate is a natural polyacid and has a unique property of gel formation in the presence of multivalent cations such as calcium ions in aqueous media, which takes place mainly at junctions in the G–G sequence-rich chain region known as the "egg box junctions." Chitosan, ([1–4] 2-amino-2-deoxy-β-D-glucan) is a naturally occurring polysaccharide comprising glucoamine and *N*-acetyl-glucoamine with unique polycation characteristics. Chitosan and alginate have been used in the pharmaceutical industry for their potential use in controlled drug delivery systems (37,38).

Drug delivery to the brain poses a major challenge due to the blood–brain barrier (BBB). The BBB, formed by brain vessel endothelial cells linked together by tight junctions, restricts the transfer of most drug substances from the bloodstream into the brain. Colloidal drug carriers such as liposomes or nanoparticles have been used to overcome this barrier (39).

Pure MA is able to cross the BBB and to diffuse into the brain tissue (40,41) whereas the MA microparticles that we prepared cannot cross through the BBB because of its higher molecular weight compared to pure MA.

One of the objectives of this study was to extend data related to MA microparticles and to prepare three different formulations of MA microparticles by using the polymers of different characteristics (Eudragit RS 100, chitosan and alginate polymers). We also aimed to prepare and determine *in vitro* characteristics and to assess the effects of MA microparticles and polymers used in their formulations on rat brain cortex DNA damage by KA, rather than its administration, which requires other methodologies.

MATERIALS AND METHODS

Materials

MA was obtained from Eczacıbaşı Pharmaceuticals Company (İstanbul, Turkey). Sodium alginate (*M*/*G*=62/38) was obtained from Sigma (USA). Eudragit RS 100 (Röhm Pharma, Germany) and Chitosan CL 213 (84% deacetylation, MW 272,000, FMC Biopolymer) were used. Triethyl citrate (TEC) was obtained by Jungbunzlauer Ladenburg. Dichloromethane (DCM) and potassium dihydrogen phosphate were purchased from Merck (Darmstadt, Germany). Sodium hydroxide was obtained from Sigma (USA). Polyvinyl alcohol (PVA; MW 14,000) was supplied by Celanese (Germany). Other substances used were all of pharmaceutical grade.

Methods

Preparation of MA Microparticles

Microsponges containing MA and Eudragit RS 100 were prepared by QESD method. In this study, we prepared MA microsponges with modification. Distilled water and PVA were used as external phase. The internal phase consisted of MA, Eudragit RS, DCM, ethyl alcohol, and TEC which was added in order to facilitate the plasticity. The amounts of polymer and TEC were kept constant and the solvent amount was 10 mL. Different ratios of drug to Eudragit RS 100 (3:1, 5:1, 7:1, 9:1) were employed to determine the effects of drug/polymer ratio on the physical characteristics and dissolution properties of microsponges (Table I). The amounts of three different external phases were chosen. Microsponges were produced with a mixing speed of 350 rpm. After adding internal phase to external phase, the mixture was continuously stirred for 2 h. Then, the mixture was filtered to separate the microsponges. The product was washed and dried at room temperature for 24 h.

Preparation of MA-loaded alginate microparticles was based on the ionotropic gelation process previously described (Table II) (9). MA-loaded chitosan microbeads were prepared according to the method of Bodmeier *et al.* (30). As can be seen in Table III, solution of chitosan (3% *w*/*w*) in dilute acetic acid (1% *v*/*v*) was dropped through a disposable syringe onto a gentle agitated thiamine pyrophosphate (TPP) solution (100 mL). The formed chitosan beads were separated after 1 h by filtration (Whatman grade 114) and washed with distilled water repeatedly. The microbeads were dried by air drying.

Table I. Formulations of MA-Loaded Eudragit Microsponges

Code	F1	F2	F3	F4	F5	F6	F7	F8	F9	F10	F11	F12
Drug/polymer ratio	3:1	5:1	7:1	9:1	3:1	5:1	7:1	9:1	3:1	5:1	7:1	9:1
External Phase (mL)	30	30	30	30	60	60	60	60	90	90	90	90
Solvent (mL)	10	10	10	10	10	10	10	10	10	10	10	10
PVA (g)	1.4	1.4	1.4	1.4	1.4	1.4	1.4	1.4	1.4	1.4	1.4	1.4
TEC (g)	0.02	0.02	0.02	0.02	0.02	0.02	0.02	0.02	0.02	0.02	0.02	0.02

Microparticle Characterization

Scanning Electron Microscopy Studies

The shape and surface characteristics of the microparticles were observed by a scanning electron microscope (Jeol JSM-6400, Japan). Samples were dusted onto double-sided tape on an aluminum stub. The stubs were then coated with gold using a cool sputter coater (Polaron E 5100) to a thickness of 250 Å.

Particle Size Determination

Sympatec Helos (HO 728; Sympatec) particle size analysis with a small sample dispersion unit was used to determine particle size and distribution.

Determination of Encapsulation Efficiency and Production Yield of MA Microparticles

The drug encapsulation efficiency was determined using the following equation:

$$\text{Drug encapsulation efficiency}\,(\%) = \text{AQ}/\text{TQ} \times 100 \qquad (1)$$

where AQ and TQ are the actual and theoretical quantity of the drug present in the MA microparticles, respectively.

The microparticles were broken in pH 7.4 phosphate buffer initially, and then drug was extracted with DCM. The residue was dissolved in 5 mL methanol after evaporation of organic phase and assayed spectrophotometrically at 285 nm. The determinations were done in triplicate.

The production yield of the microparticles was determined by calculating accurately the initial weight of the raw materials and the last weight of the microparticles obtained.

In Vitro Release Studies of MA Microparticles

Dissolution studies of MA microparticles were carried out by using USP XXV paddle method at 37±0.5°C (PharmaTest PTWII dissolution apparatus) under sink conditions. The MA powder (<100 mesh) or microparticles (equivalent to 20 mg MA) were placed into 400 mL of a dissolution medium (pH 7.4 phosphate buffer) and rotated at 50 rpm. At preset time intervals, aliquots were withdrawn and replaced by an equal volume of fresh dissolution medium to maintain constant volume. After suitable dilution, the samples were analyzed spectrophotometrically at 285 nm (Shimadzu UV-1208). All experiments were repeated three times.

The mathematical models, first-order (diss (%)=100(1−e^{-kt})), Higuchi ($diss\,(\%) = kt_{50\%}$), and Weibull ($diss\,(\%) = 100\left(1 - e^{-(t/T_d)\beta}\right)$) equations were fitted to individual dissolution data with linear regression by SPSS 9.0 for Windows (Tables IV and V) (42–44).

Table II. Formulations of the Alginate Beads Utilizing 3×2^2 Factorial Design (9)

Code	X_1	X_2	X_3	Y_1	Y_2
A1	1:2	0.2	3	1.45	79.3
A2	1:2	0.2	12	2.02	97.67
A3	1:2	0.7	3	1.27	83.45
A4	1:2	0.7	12	1.67	92.14
A5	1:1	0.2	3	0.79	91.28
A6	1:1	0.2	12	2.93	95.67
A7	1:1	0.7	3	1.65	96.56
A8	1:1	0.7	12	1.78	91.63
A9	2:1	0.2	3	0.85	97.45
A10	2:1	0.2	12	5.22	98.58
A11	2:1	0.7	3	1.54	95.27
A12	2:1	0.7	12	0.9	98.99

X_1 drug/polymer ratio, X_2 $CaCl_2$ concentration (M), X_3 curing time (in hours), Y_1 the time for 50% of the drug to be released ($t_{50\%}$; in hours), Y_2 percent drug entrapment efficiency of the beads

In Situ Studies

Determination of DNA Damage. Adult Sprague–Dawley rats weighing 300–350 g were used for the present study. All animals were maintained on a 12:12-h dark–light cycle with free access to chow and water. The protocol for the experiment was approved by the Appropriate Animal Care

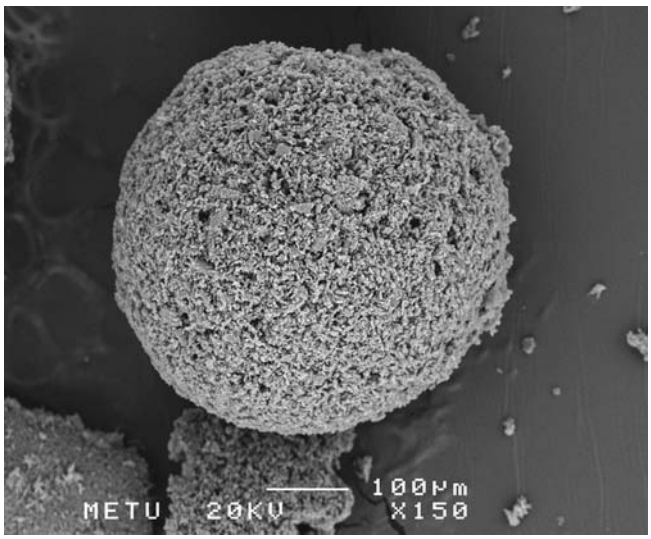

Fig. 2. Scanning electron photograph of the MA-loaded Eudragit microsponge formulation coded F11

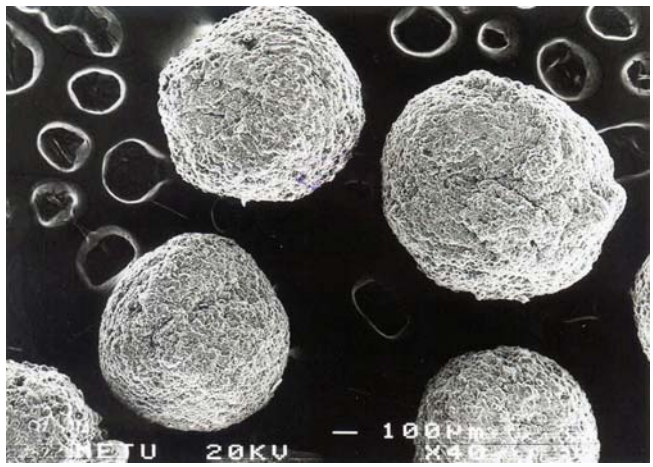

Fig. 3. Scanning electron photograph of the MA-loaded alginate bead formulation coded A10

Table III. Preparation Parameters of MA-Loaded Chitosan Microparticles

Formulation codes	Drug/polymer ratio	TPP concentration
C1	1:1	0.5
C2	1:1	1
C3	2:1	0.5
C4	2:1	1
C5	3:1	0.5
C6	3:1	1

Committee of Ege University. Rats were decapitated, the brains removed, and the cortex samples dissected on ice. DNA was extracted from the brain cortex using Trizol reagent (Gibco BRL Life Technologies) based on phenol–chloroform precipitation. The concentration of DNA was determined by measuring the absorbance at A260. Purity of DNA was also checked by the ratio of absorbance at A260/A280.

Ten percent of tissue homogenates were prepared using ice-cold HEPES buffer (40 mM, pH 7.0). The homogenate (80 μL) in 40 mM HEPES buffer was incubated with kainate (1 mM) in the presence of rat cortex DNA (5 μg) with or without MA (1 mM), MA microsponge, and polymer at 37°C for 90 min. The final volume was 100 μL. After incubation, reaction was stopped with 5 μL of 0.25% bromophenol blue. The mixtures were centrifuged at 9,000×*g* for 15 min and supernatants were used for agarose gel analysis.

Agarose gel electrophoresis was performed with conditions at 75 V on 1.2% agarose in Tris–acetate–EDTA buffer system for 90 min. Following electrophoresis, gel was stained with ethidium bromide irradiated from below with a UV transilluminator box and photographed. DNA damage was quantified from gel photographs using the Biocapt software (Vilber Lourmat, France).

Statistical Analysis

The mean values±standard deviations (SD) of at least three independent experiments in all cases were analyzed using SPSS for Windows (Version 12.0). Differences between groups were analyzed by one-way analysis of variance.

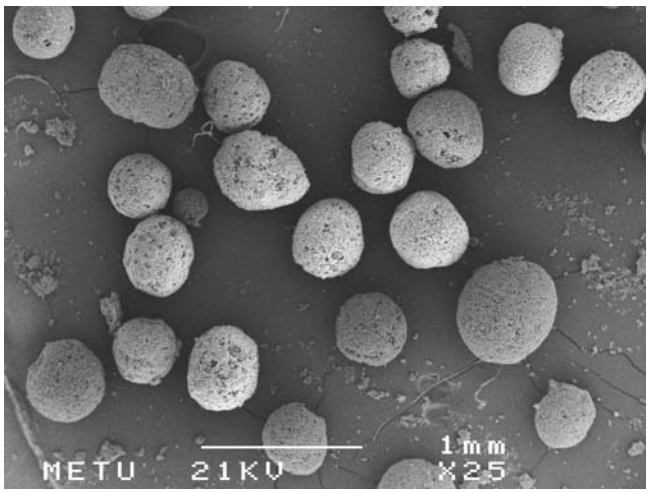

Fig. 4. Scanning electron photograph of the MA-loaded chitosan microparticle formulation coded C5

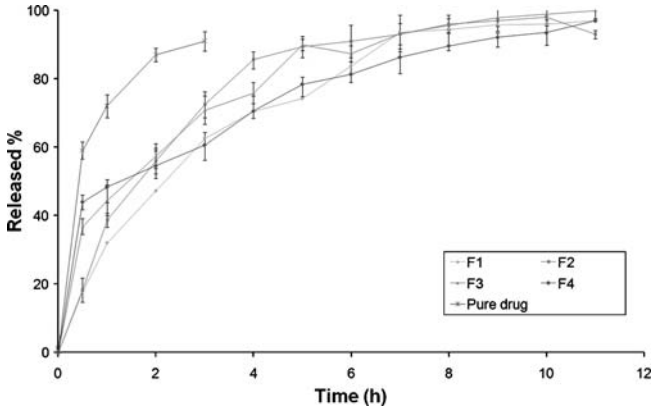

Fig. 5. The release profiles of Eudragit microparticles prepared by using 30 mL external phase. *Error bars* represent 95% confidence intervals (n=3)

RESULTS AND DISCUSSION

Characterization of MA Microparticles

The mean particle size of 12 formulations **(**F1–F12**)** of Eudragit microsponges were between 0.407±0.1 and 0.593± 0.1 mm (mean±confidence interval $t_{95\%}$).

In this study, the morphology of the Eudragit microsponges prepared by QESD method was investigated by scanning electron microscopy (SEM). The scanning electron photograph of the microsponges is shown in Fig. 2. It was observed by SEM analysis that the microsponges were finely spherical and uniform. Microscopy studies showed that MA microsponges contained pores. These findings are similar to the results reported previously (23,24,27).

The mean particle size of alginate formulations (A1–A12) were between 0.997±0.1 and 1.436±0.2 mm (mean±confidence interval $t_{95\%}$). The composition of each MA-loaded alginate microparticle formulation prepared is given Table II. The surface photographs of MA–alginate microparticles were shown in our previous study (9). The alginate microparticles prepared were found to be discrete and spherical (Fig. 3). When the alginate microparticles were prepared by using 0.7 M $CaCl_2$ solution (high concentration) as a cross-linking agent, cracks and fissures were observed on the surface of the microparticles.

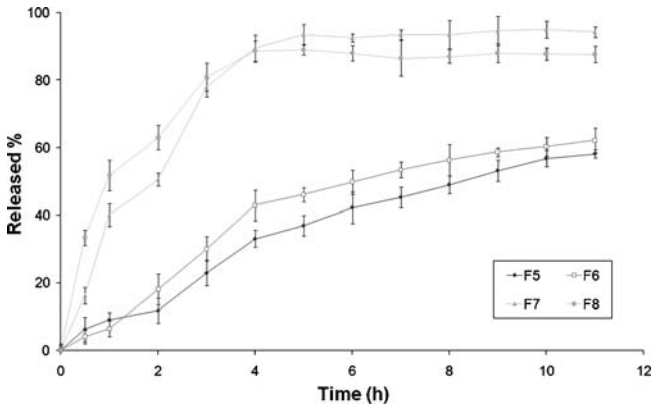

Fig. 6. The release profiles of Eudragit microparticles prepared by using 60 mL external phase. *Error bars* represent 95% confidence intervals (n=3)

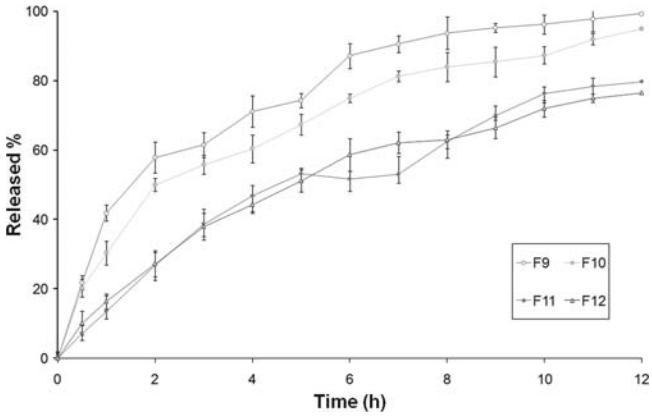

Fig. 7. The release profiles of Eudragit microparticles prepared by using 90 mL external phase. *Error bars* represent 95% confidence intervals (n=3)

The mean particle size of chitosan formulations (C1–C6) were between 0.497±0.1 and 0.753±0.2 mm (mean±confidence interval $t_{95\%}$). The composition of each MA-loaded chitosan microparticle formulation prepared is given Table III. The surface photograph of MA-loaded chitosan microbeads is illustrated in Fig. 4. The SEM photographs exhibited that the shape of these microbeads was not completely spherical and porous. Some researchers reported that the matrix structure depended on the method of drying (30). In this study, the shape of the microbeads in wet state was very spherical and, even after air drying, the beads shrank and had a porous surface.

Encapsulation Efficiency and *In Vitro* Release of MA Microparticles

The production yield was between 73.2% and 79.3% for 12 Eudragit microsponges **(**formulations coded F1–F12**)**. The actual drug content of microsponges, expressed as a percentage of the amount of MA entrapped in the microsponges, varied between 66.7% and 73.4% for 12 Eudragit microsponges. The encapsulation efficiency was found high in all formulations since it exceeded 90%.

The release profiles of Eudragit microsponges are shown in Figs. 5, 6, and 7. The microsponges prepared from 90 mL external phase gave rise to a better modified release up to 12 h when compared to the ones prepared with either 30 or 60 mL. On the other hand, MA release rates from Eudragit microsponges with 7:1 and 9:1 drug/polymer ratios were slow whereas release rates from Eudragit microsponges with 3:1 and 5:1 drug/polymer ratios were faster. The present study showed that, generally, an increase in the ratio of drug/polymer resulted in a reduction in release of MA from Eudragit microsponges (Figs. 5, 6, and 7). Previously published data have shown similar findings (27).

This study shows that both drug/polymer ratio and external phase volume have important effects on drug release of MA-loaded Eudragit microsponges.

According to our kinetic evaluations, the suitable formulations were found as formulation codes F11 and F12 (containing 90 mL external phase and 7:1 or 9:1 drug/polymer ratios) and their release profiles fitted into Weibull distribution (44) (Tables IV and V). When the release kinetics of Eudragit microsponges (formulations coded F11 and F12) were investigated, it was seen that the drug release from all microsponges was found to follow Weibull distribution, as shown in Tables IV and V.

The *in vitro* release profiles of MA from alginate beads are shown in Figs. 8 and 9. Ninety-seven percent of MA is released from the alginate bead formulation **(**formulation coded A10**)** into the phosphate buffer (pH 7.4) dissolution medium during the 9 h. According to kinetic evaluations, the zero order kinetic model provides a better fit to the release data for optimum formulation coded A10 (9).

The yield of MA-loaded alginate beads ranged from 71% to 89% and the encapsulation efficiency was determined between 79.3% and 98.9%. The encapsulation efficiency of all formulations was high due to water-insoluble properties of MA (45). The percent drug loading of 12 alginate bead formulations(A1–A12) ranged between 49.7±1.3 and 57.3±1.7(mean±confidence interval $t_{95\%}$) while the actual drug content varied between 5 and 5.7 mg in a 10-mg bead sample. The high $CaCl_2$ concentration causes rapid release of MA from matrices due to the performed cracks and fissures previously reported in our study (9).

Table IV. Parameters of the Mathematical Models and Descriptive Statistics of Regression for the Dissolution Data of Formulation F1 to F6 with Paddle Method

Model	Statistics	F1	F2	F3	F4	F5	F6
First order	r^2	0.907	0.943	0.787	0.748	0.893	0.913
	k	3.067×10^{-2}	2.391×10^{-3}	1.924×10^{-2}	3.127×10^{-3}	2.095×10^{-3}	3.012×10^{-2}
	SE	0.003	0.002	0.003	0	0	0.005
	RMS	0.117	0.947	0.714	0.189	9.659×10^{-2}	0.213
Higuchi	r^2	0.903	0.703	0.899	0.793	0.814	0.895
	k	9.189	3.521	7.741	3.479	3.102	9.182
	SE	0.543	0.395	0.649	0.339	0.227	0.436
	RMS	127.13	229.7	149.3	183	132.7	167.4
Weibull	r^2	0.957	0.895	0.912	0.971	0.913	0.949
	T_d	236.7	280.4	284.4	247.7	186.3	147.1
	β	0.613	0.712	0.931	0.583	0.557	0.624
	SE	0.08	0.053	0.123	0.033	0.037	0.513
	RMS	5.583×10^{-3}	2.33×10^{-2}	3.067×10^{-2}	2.315×10^{-2}	3.513×10^{-3}	2.042×10^{-3}

r^2 determination coefficient, *RMS* residual mean square, *SE* standard error of model parameters, k dissolution rate constant, β shape parameter, T_d time at which 63.2 of the material dissolved (in minutes)

Table V. Parameters of the Mathematical Models and Descriptive Statistics of Regression for the Dissolution Data of Formulation F7 to F12 with Paddle Method

Model	Statistics	F7	F8	F9	F10	F11	F12
First order	r^2	0.793	0.852	0.893	0.894	0.867	0.919
	k	4.192×10^{-3}	1.903×10^{-3}	3.116×10^{-3}	2.219×10^{-2}	3.993×10^{-2}	3.153×10^{-3}
	SE	0.003	0.004	0.001	0.001	0.002	0.002
	RMS	0.764	0.546	0.713	0.273	9.591×10^{-2}	9.873×10^{-2}
Higuchi	r^2	0.934	0.863	0.919	0.904	0.941	0.927
	k	3.985	8.741	4.479	3.107	7.776	3.422
	SE	0.387	0.749	0.366	0.298	0.637	0.763
	RMS	232.2	187.2	137.5	227.3	177.3	196.4
Weibull	r^2	0.981	0.971	0.973	0.987	0.989	0.993
	T_d	1287.8	1469.6	273.7	341.9	563.3	579.7
	β	0.883	0.931	0.871	0.697	0.573	0.728
	SE	0.109	0.298	0.547	0.368	0.3 01	0.103
	RMS	6.353×10^{-2}	3.016×10^{-2}	4.121×10^{-2}	7.71×10^{-2}	2.571×10^{-2}	2.117×10^{-2}

r^2 determination coefficient, *RMS* residual mean square, *SE* standard error of model parameters, k dissolution rate constant, β shape parameter, T_d time at which 63.2 of the material dissolved (in minutes)

A suitable controlled release dosage form of MA–alginate microparticles can be prepared with formulation A10 according to the optimization of the process using 3×2^2 factorial design. The experimental parameters of formulation A10 are 2:1 drug to polymer ratio, 0.2 M $CaCl_2$ solution as cross-linking agent, and a 12-h curing time. Entrapment efficiency and drug release ($t_{50\%}$) value of formulation A10 are 98.58% and 5.22 h, respectively (9).

A fairly high yield (69–77%) of MA-loaded chitosan microbeads was obtained. Their encapsulation efficiencies were in the range of 67.9–74.7%. The percent drug loading of microbead formulations (C1–C6) ranged between 29.7±1.1 and 39.3±1.3 (mean±confidence interval $t_{95\%}$) while the actual drug content varied between 3 and 4 mg in a 10-mg microbead sample.

In the present investigation, chitosan microbeads containing MA were prepared by dropping drug containing chitosan solutions into tripolyphosphate solutions. The interaction of the positively charged chitosan molecules with the anionic counterion, tripolyphosphate, caused the formation of gelled spheres. *In vitro* release profiles of MA from chitosan microbeads are shown in Fig. 10.

Drug to polymer ratios and TPP concentrations were investigated as preparative variables. Due to the ionic nature of the cross-linking, the charge density of chitosan, the drug to polymer ratio, and TPP under preparation conditions would be expected to affect bead formation.

Chitosan microbeads were prepared in the ratios of 1:1, 2:1, and 3:1 (drug/polymer). The most convenient ratio was found to be 3:1 as this formulation exhibited a prolonged release up to 5.5 h. A small variation from the TPP concentration in the gelling medium did not markedly affect the encapsulation efficiency. The drug release varied insignificantly with increasing TPP concentrations. Previously published data have shown similar findings (32).

As seen in Figs. 7, 8, and 10 and Tables I, II, III, IV, and V, the release and kinetic evaluations of the individual formulations on the basis of kinetics for releasing MA showed that the C5 (5 h, 63.4%), A10 (9 h, 97%), and F11 (12 h, 73.9%) among the chitosan, alginate, and Eudragit micropar-

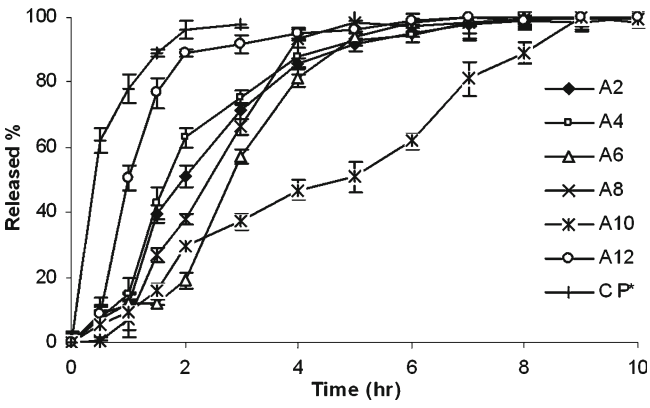

Fig. 8. The release profiles of alginate beads prepared by using 0.2 and 0.7 M $CaCl_2$ solution with different drug/polymer ratios at 12 h. *CP* commercial product. *Error bars* represent 95% confidence intervals

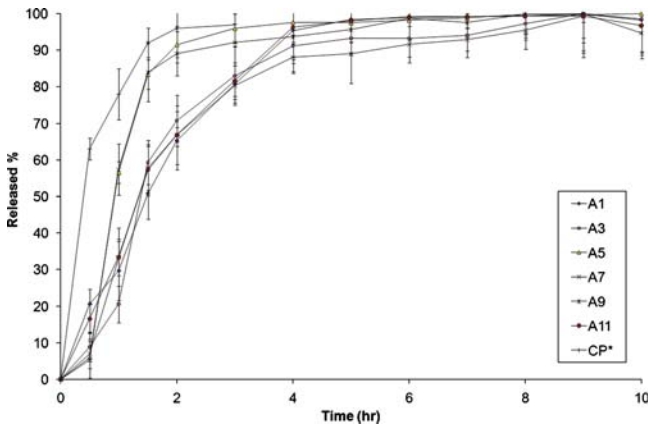

Fig. 9. The release profiles of alginate beads prepared by using 0.2 and 0.7 M $CaCl_2$ solution with different drug/polymer ratios at 3 h. *CP* commercial product. *Error bars* represent 95% confidence intervals

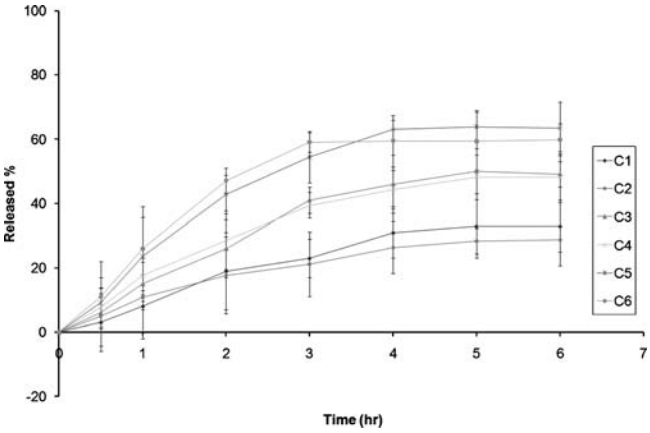

Fig. 10. The release profiles of MA-loaded chitosan microbeads

ticle formulations, respectively, gave rise to the most convenient parameters. We, therefore, propose the alginate microparticles better drug carrier as it fitted almost zero order kinetics.

Kinetic data obtained from *in vitro* dissolution tests were analyzed according to different mathematical models. After fitting these models, the selection was based on the comparison of higher determination coefficients and smaller mean square (Tables IV and V). Higher determination coefficients and lower residual mean square data were obtained from Weibull distribution with its parameters describing the types of dissolution profiles and dissolution time. The shaper parameter β characterizes the profile as either exponential (β=1), s-shaped with upward curvature followed by a turning point (β>1), or as one with steeper initial slope than consistent with the exponential (β<1). All β values were less than 1. The time parameter, T_d, represents the time interval necessary to dissolve 63.2% of the drug substance (44). The time parameters of formulations coded F11 and F12 was found as 563.3 and 579.7 min, respectively. According to kinetic evaluations, the Weibull kinetic model provides a better fit to the release data for F11 and F12 microparticle formulations.

In Situ Studies

Figure 11a, b shows the effect of MA, MA microsponges, and Eudragit polymer used in MA microsponge preparations on the rat cortex brain DNA damage. According to our comparative results, DNA damage was observed as the

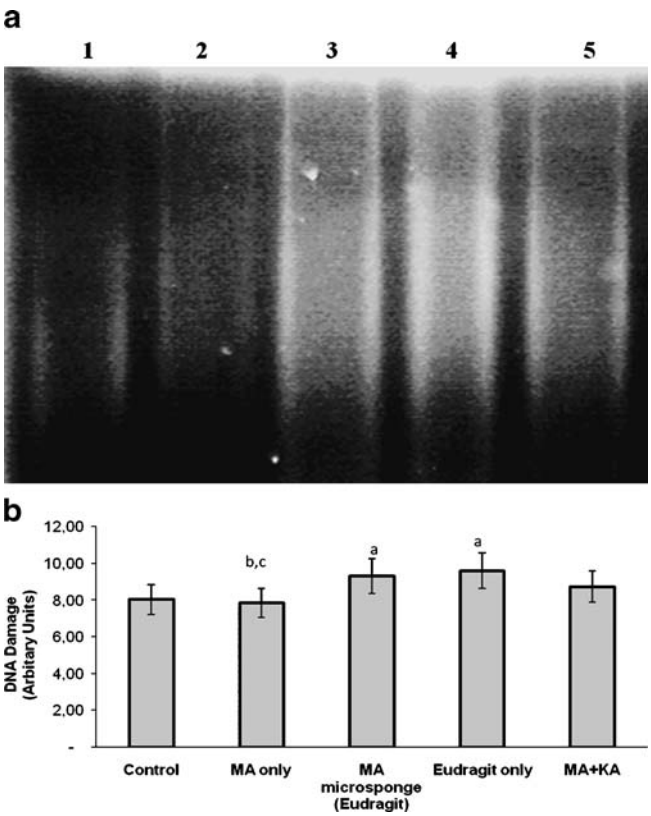

Fig. 11. a Ethidium bromide-stained agarose gel of supernatants. *Lane 1* control (rat cortex DNA without any treatment), *lane 2* MA only (3 mg), *lane 3* MA-loaded (equivalent to 3 mg MA) Eudragit microsponges, *lane 4* Eudragit polymer only, *lane 5* KA (1 mM)+MA (3 mg). **b** Quantitative analysis of DNA fragmentation detected in rat brain cortex DNA samples treated with MA, MA-loaded Eudragit microsponges, and Eudragit polymer. Values in **b** are the mean±SEM. Experiments were performed for three times. $^{a}p<0.05$ *vs* control; $^{b}p<0.05$ *vs* Eudragit only; $^{c}p<0.05$ *vs* MA-loaded Eudragit microsponges

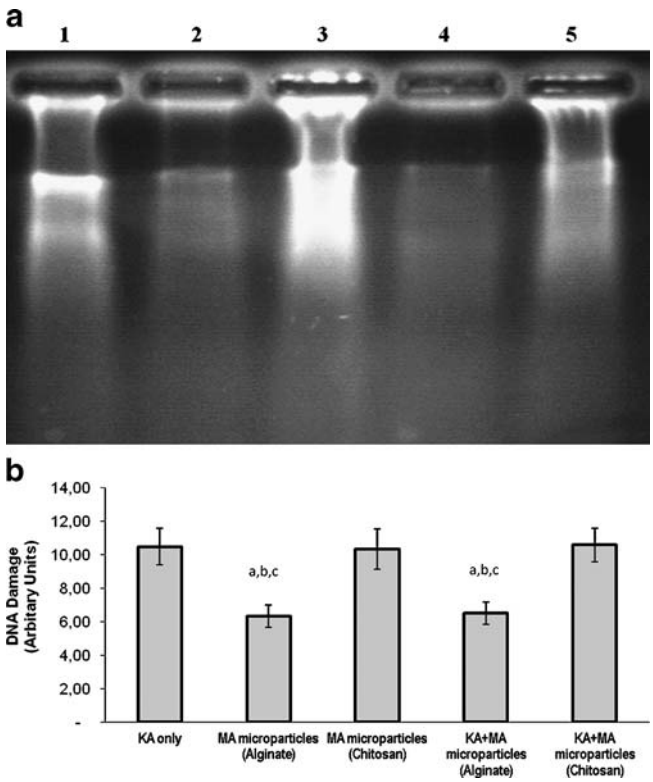

Fig. 12. a Ethidium bromide-stained agarose gel of supernatants. *Lane 1* KA only (1 mM), *lane2* MA-loaded (equivalent to 3 mg MA) alginate microparticles only, *lane 3* MA-loaded (equivalent to 3 mg MA) chitosan microparticles only, *lane 4* KA (1 mM)+MA-loaded (equivalent to 3 mg MA) alginate microparticles, *lane 5* KA (1 mM) +MA-loaded (equivalent to 3 mg MA) chitosan microparticles. **b** Quantitative analysis of DNA fragmentation detected in rat brain cortex DNA samples treated with MA, MA microparticles, and polymers used. Values in **b** are the mean±SEM. Experiments were performed for three times. $^{a}p<0.05$ *vs* KA only; $^{b}p<0.05$ *vs* MA-loaded chitosan microparticles, $^{c}p<0.05$ *vs* KA+MA-loaded chitosan microparticles

degradation of DNA in all experimental samples treated with MA microsponges, Eudragit, and KA. However, the levels of DNA damage were significantly high in MA microsponges with Eudragit or Eudragit only when compared with untreated control and MA only ($p<0.05$). Our results clearly showed that MA only treatment has no effect on damage DNA. MA+KA treatment also caused DNA damage but this effect was nonsignificant when compared with untreated control, MA (3 mg) only, MA-loaded Eudragit microsponges (equivalent to 3 mg MA), and Eudragit polymer only. Therefore, it can be suggested that Eudragit RS, as an acrylic polymer used in the preparations of MA microsponges, has relatively harmful effect on rat brain cortex DNA.

Figure 12a, b shows the effect of MA, MA microparticles, and alginate and chitosan polymers used in MA microparticle formulations on the rat cortex brain DNA damage. Our results indicate that DNA damage was significantly low in MA microparticles with alginate only treatment when compared with KA only ($p<0.05$). Similarly, the levels of DNA damage were significantly decreased in KA+MA with alginate treatment when compared to MA-loaded (equivalent to 3 mg MA) chitosan microparticles ($p<0.05$), or KA+MA microparticles with chitosan ($p<0.05$). Accordingly, it can be assumed that chitosan polymer is more harmful for DNA than alginate polymer, and this polymer may limit the protective effect of MA in a microparticle formulation on DNA damage.

Taken together, the present study reveals the preparation and *in vitro* characteristics of MA-loaded biodegradable alginate or chitosan microparticle formulations as well as modified release of MA microsponges with acrylic polymer, Eudragit RS 100. Our results showed that alginate microparticles gave rise to a diminished DNA damage when compared to chitosan and Eudragit RS 100. However, because of the inability of MA microparticles to cross the BBB, our formulation system can be modified to yield MA microparticles or nanoparticles to be used in optimal delivery systems. Altogether, these works address an important foundation for the future studies into improving devices for brain drug delivery.

ACKNOWLEDGEMENTS

This study was supported by a research grant from Ege University (2003/ECZ/011). The authors thank Eczacıbaşı Pharmaceuticals Company, Istanbul, Turkey for kindly supplying the MA powder. We would like to thank Dr. Cengiz Tan from the Middle East Technical University (METU) for taking the scanning electron microphotographs. We would also like to thank Assoc. Prof. Dr. Zelihagül Değim from the Faculty of Pharmacy, Gazi University for her help for determining particle size.

REFERENCES

1. L. Fang, S. Numajiri, D. Kobayashi, H. Ueda, K. Nakayama, H. Miyamae, and Y. Morimoto. Physicochemical and crystallographic characterization of mefenamic acid complexes with alkanolamines. *J. Pharm. Sci*. **93**:144–154 (2004).
2. Y. Joo, H. Kim, R. Woo, C. Park *et al.* Mefenamic acid shows neuroprotective effects and improves cognitive impairment in *in vitro* and *in vivo* Alzheimer's disease models. *Mol. Pharmacol.* **69**:76–84 (2006).
3. J. E. F. Reynolds. *Martindale: The Extra Pharmacopoeia*, 31rd ed., The Pharmaceutical Press, London, 1998, pp. 58–59.
4. M. G. Jelen, D. Jamnig, H. Schabus, W. Pipam, and R. Likar. A comparison of the efficacy and rate of side-effects of mefenamic acid and naproxen in adult patients following elective tonsillectomy: a randomized double-blind study. *Acute Pain* in press (2008).
5. J. K. Lalla, and P. L. Ahuja. Drug targeting using non-magnetic and magnetic albumin-globulin mix microspheres of mefenamic acid. *J. Microencapsul*. **8**:37–52 (1991).
6. F. Sevgi, M. Ozyazıcı, B. Kaynarsoy, D. Ozyurt, and C. Pekçetin. *Histological evaluation of drug-loaded alginate beads and Eudragit microspheres*. Proceedings of the 13th Inter. Pharm. Technol. Symp., 10–13 Sept., 2006, Antalya, Turkey, pp. 135–136.
7. F. Sevgi, B. Sarpaş, and A. Yurdasiper. *The effect of tabletting on the release characteristics of mefenamic acid microspheres*. European Conference on Drug Delivery and Pharmaceutical Technology, 10–12 May, 2004, Sevilla, Spain, p. 326.
8. S. Gungor, A. Yıldız, Y. Ozsoy, E. Cevher, and A. Araman. Investigations on mefenamic acid sustained release tablets with water-insoluble gel. *Farmaco*. **58**:397–401 (2003).
9. F. Sevgi, B. Kaynarsoy, and G. Ertan. An antiinflammatory drug (mefenamic acid) incorporated in biodegradable alginate beads: development and optimization of the process using factorial design. *Pharm. Dev. Technol*. **13**(1):5–13 (2008).
10. FDA/CDER. Waiver of *in vivo* bioavailability and bioequivalance studies for immediate release solid oral dosage forms based on a biopharmaceutics classification system. *Guidance for Industry*, August, 2000.
11. G. Kimura, G. Betz, and H. Leuenberger. Influence of loading volume of mefenamic acid on granules and tablet characteristics using a compaction simulator. *Pharm. Dev. Technol*. **12**:627–635 (2007).
12. T. A. Tokumura. A screening system of solubility for drug design and discovery. *Pharm. Technol. Japan*. **16**(13):19–27 (2000).
13. M. Yazdanian, K. Briggs, C. Jankovsky, and A. Hawi. The "high solubility" definition of the current FDA guidance on biopharmaceutical classification system may be too strict for acidic drugs. *Pharm. Res*. **21**(2):293–299 (2004).
14. M. S. Y. Khan, and M. Akhter. Glyceride derivatives as potential prodrugs: synthesis, biological activity and kinetic studies of glyceride derivatives of mefenamic acid. *Pharmazie*. **60**(2):110–114 (2005).
15. F. Sevgi, B. Kaynarsoy, M. Ozyazici, Ç. Pekcetin, and D. Özyurt. A comparative histological study of alginate beads as a promising controlled release delivery for mefenamic acid. *Pharm. Dev. Technol*. **13**(5):387–392 (2008).
16. M. Asanuma, S. Nishibayashi-Asanuma, I. Miyazaki, M. Kohno, and N. Ogawa. Neuroprotective effects of nonsteroidal anti-inflammatory drugs by direct scavenging of nitric oxide radicals. *J. Neurochem*. **76**:1895–1904 (2001).
17. G. M. Kasof, A. Mandelzys, S. D. Maika, and R. E. Hammer. Kainic acid-induced neuronal death is associated with DNA damage and a unique immediate-early gene response in c-*fos*–lacZ transgenic rats. *J. Neurosci*. **15**(6):4238–4249 (1995).
18. H. A. Yamamoto, and P. V. Mohanan. Effect of alpha-ketoglutarate and oxaloacetate on brain mitocondrial DNA damage and seizures induced by kainic acid in mice. *Toxicol. Lett*. **143**(2):115–122 (2003).
19. Y. Kawashima, T. Niwa, T. Handa, H. Takeuchi, T. Iwamoto, and K. Itoh. Preparation of controlled release microspheres of ibuprofen with acrylic polymers by a novel quasi-emulsion solvent diffusion method. *J. Pharm. Sci*. **78**:68–72 (1989).
20. Y. Kawashima, T. Niwa, T. Handa, H. Takeuchi, T. Hino, and Y. Ito. Control of prolonged drug release and compression properties of ibuprofen microsponges with acrylic polymer, Eudragit RS by changing their intraparticle porosity. *Chem. Pharm. Bull.* **40**:196–201 (1992).
21. F. Cui, M. Yang, Y. Jiang, D. Cun, W. Lin, Y. Fan, and Y. Kawashima. Design of sustained-release nitrendipine microspheres having solid dispersion structure by quasi-emulsion solvent diffusion method. *J. Control. Release*. **91**:375–384 (2003).

22. D. Perumal. Microencapsulation of ibuprofen and Eudragit RS 100 by the emulsion solvent diffusion technique. *Int. J. Pharm.* **218**:1–11 (2001).
23. T. Çomoğlu, N. Gönül, and T. Baykara. Preparation and *in vitro* evaluation of modified release ketoprofen microsponges. *Farmaco*. **58**:101–106 (2003).
24. M. Orlu, E. Cevher, and A. Araman. Design and evaluation of colon spesific drug delivery system containing flurbiprofen microsponges. *Int. J. Pharm.* **318**:103–117 (2006).
25. S. Nacht, and M. Katz. The microsponge: a novel topical programmable delivery system. In D. W. Osborne, and A. H. Aman (eds.), *Topical Drug Delivery Formulations*, Marcel Dekker, New York, 1990, pp. 299–325.
26. K. Embil, and S. Nacht. The microsponge® delivery system (MDS): a topical delivery system with reduced irritancy incorporating multiple triggering mechanisms for the release of actives. *J. Microencapsul.* **13**:575–588 (1996).
27. M. Jelvahgari, M. R. Siahi-Shadbad, S. Azarmi, P. Martin Gary, and A. Nokhodchi. The microsponge delivery system of benzoil peroksit: preparation, characterization and release studies. *Int. J. Pharm.* **308**:124–132 (2006).
28. A. Yurdasiper, B. Kaynarsoy, and F. Sevgi. *Preparation of flurbiprofen microsponges formulated in different gels and evaluation of antiinflammatory activity*. 3rd World Congress of the Board of Pharmaceutical Sciences of FIP, Amsterdam, The Netherlands, 22–25 April, 2007, p. PSWC07L_ 1183.
29. A. Yurdasiper, B. Kaynarsoy, and F. Sevgi. *Preparation and dissolution kinetics of mefenamic acid microsponges*. 8th Inter. Symp. on Pharm. Scien. (ISOPS-8), 13–16 June, 2006, Ankara, Turkey, number 91, p. 363.
30. R. Bodmeier, K. H. Oh, and Y. Pramar. . Preparation and evaluation of drug-containing chitosan beads. *Drug Dev. Ind. Pharm.* **15**:1475–1494 (1989).
31. B. Arıca, S. Çalış, P. Atilla, N. T. Durlu, N. Çakar, H. S. Kaş, and A. A. Hıncal. *In vitro* and *in vivo* studies of ibuprofen-loaded biodegradable alginate beads. *J. Microencapsul.* **22**(2):153–165 (2005).
32. M. Çetin, İ. Vural, Y. Çapan, and A. A. Hıncal. *Effects of manufacturing parameters on the characteristics of the famotidine loaded chitosan beads and microspheres*. Proceedings of the 12th Inter. Pharm. Technol. Symp. (IPTS-2004), 12–15 Sept., 2004, İstanbul, Turkey, pp. 109–110.
33. Eudragit Data Sheeets, Röhm Pharma GmbH, Darmstadt, 1991.
34. D. L. Kaplan, B. J. Wiley, J. M. Mayer, S. Arcidiacono, J. Keith, S. J. Lombardi, D. Ball, and A. L. Allen. In S. W. Shalaby (eds.), *Biomedical polymers: designed-to-degrade systems*. Hanser Publishers, New York, NY, 1994, Biosynthetic polysaccharides, pp. 189–212.
35. W. R. Gombotz, and S. F. Wee. Protein release from alginate matrices. *Adv. Drug Deliv. Rev.* **31**:267–285 (1998).
36. L. Illum. Chitosan and its use as a pharmaceutical excipient. *Pharm. Res.* **15**:1326–1331 (1998).
37. X. Z. Shu, and K. J. Zhu. The release behavior of brilliant blue from calcium-alginate gel beads coated by chitosan: the preparation method effect. *Eur. J. Pharm. Biopharm.* **53**:193–201 (2002).
38. C. M. Silva, J. A. Ribeiro, M. Figueiredo, D. Ferreira, and F. Veiga. Microencapsulation of hemoglobin in chitosan-coated alginate microspheres prepared by emulsification/internal gelation. *AAPS J.* **7**(4):E903–E913 (2006).
39. K. Ulbrich, T. Hekmatara, E. Herbert, and J. Kreuter. Transferrin- and transferrin-receptor-antibody-modified nanoparticles enable drug delivery across the blood–brain barrier (BBB). *Eur. J. Pharm. Biopharm.* in press (2008).
40. A. Hernandez, C. Paeile, H. Perez, S. Ruiz, and R. Soto Moyano. Cortical facilitatory effect of mefenamic acid. *Arch. Int. Pharmacodyn. Ther.* **244**(1):100–106 (1980).
41. M. Zhang, W. J. Shi, X. W. Fei, Y. R. Liu, and X. M. Zeng. Mefenamic acid bi-directionally modulates the transient outward K+ current in rat cerebellar granule cells. *Toxicol. Appl. Pharmacol.* **226**(3):225–235 (2008).
42. T. Higuchi. Mechanism of sustained-action medication: theoretical analysis of rate of release of solid drug dispersed in solid matrices. *J. Pharm. Sci.* **52**:1145–1149 (1963).
43. M. Gibaldi, and S. Feldman. Establishment of sink conditions in dissolution rate determinations, Theoretical considerations and application to non-disintegrating dosage forms. *J. Pharm. Sci.* **56**:1238–1242 (1967).
44. F. Langenbucher. Linearization of dissolution rate curves by the Weibull distribution. *J. Pharm. Pharmacol.* **24**:979–981 (1972).
45. R. Bodmeier, and J. Wang. Microencapsulation of drugs with aqueous colloidal polymer dispersions. *J. Pharm. Sci.* **82**:191–194 (1993).